remote sensing

MDPI

Article

Integration of Ground-Based Remote-Sensing and In Situ Multidisciplinary Monitoring Data to Analyze the Eruptive Activity of Stromboli Volcano in 2017–2018

Flora Giudicepietro [1,*], Sonia Calvari [2], Salvatore Alparone [2], Francesca Bianco [1], Alessandro Bonaccorso [2], Valentina Bruno [2], Teresa Caputo [1], Antonio Cristaldi [2], Luca D'Auria [3], Walter De Cesare [1], Bellina Di Lieto [1], Antonietta M. Esposito [1], Salvatore Gambino [2], Salvatore Inguaggiato [4], Giovanni Macedonio [1], Marcello Martini [1], Mario Mattia [2], Massimo Orazi [1], Antonio Paonita [4], Rosario Peluso [1], Eugenio Privitera [2], Pierdomenico Romano [1], Giovanni Scarpato [1], Anna Tramelli [1] and Fabio Vita [4]

1 Istituto Nazionale di Geofisica e Vulcanologia, Osservatorio Vesuviano, 80124 Napoli, Italy
2 Istituto Nazionale di Geofisica e Vulcanologia, Osservatorio Etneo, 95125 Catania, Italy
3 Instituto Volcanológico de Canarias (INVOLCAN), 38320 San Cristobal de La Laguna, Tenerife, Spain
4 Istituto Nazionale di Geofisica e Vulcanologia, Sezione di Palermo, 90146 Palermo, Italy
* Correspondence: flora.giudicepietro@ingv.it; Tel.: +39-081-610-8326

Received: 5 July 2019; Accepted: 31 July 2019; Published: 2 August 2019

Abstract: After a period of mild eruptive activity, Stromboli showed between 2017 and 2018 a reawakening phase, with an increase in the eruptive activity starting in May 2017. The alert level of the volcano was raised from "green" (base) to "yellow" (attention) on 7 December 2017, and a small lava overflowed the crater rim on 15 December 2017. Between July 2017 and August 2018 the monitoring networks recorded nine major explosions, which are a serious hazard for Stromboli because they affect the summit area, crowded by tourists. We studied the 2017–2018 eruptive phase through the analysis of multidisciplinary data comprising thermal video-camera images, seismic, geodetic and geochemical data. We focused on the major explosion mechanism analyzing the well-recorded 1 December 2017 major explosion as a case study. We found that the 2017–2018 eruptive phase is consistent with a greater gas-rich magma supply in the shallow system. Furthermore, through the analysis of the case study major explosion, we identified precursory phases in the strainmeter and seismic data occurring 77 and 38 s before the explosive jet reached the eruptive vent, respectively. On the basis of these short-term precursors, we propose an automatic timely alarm system for major explosions at Stromboli volcano.

Keywords: Stromboli volcano; multidisciplinary monitoring of volcanoes; explosive eruptions; volcano ground-based remote sensing; volcanic risk mitigation; experimental geophysics; volcano timely alarm; strainmeter

1. Introduction

Stromboli is the northernmost island of the Aeolian Arc, in the Mediterranean Sea (Italy; Figure 1, inset), with persistent eruptive activity typically characterized by 5–20 Strombolian explosions per hour [1]. A large amount of gas is continuously emitted through several small eruptive vents [2–4] located in the crater zone (Figure 1). The position of the vents varies over time, but there are three areas where the main vents are typically located [5,6]: The northeast (NE), central (C) and southwest (SW) areas (Figure 1, right). The structural setting of Stromboli is controlled by the "Sciara del Fuoco"

flank depression (SdF, Figure 1), which is the result of several sector-collapses of the northwestern slope of the island [7,8].

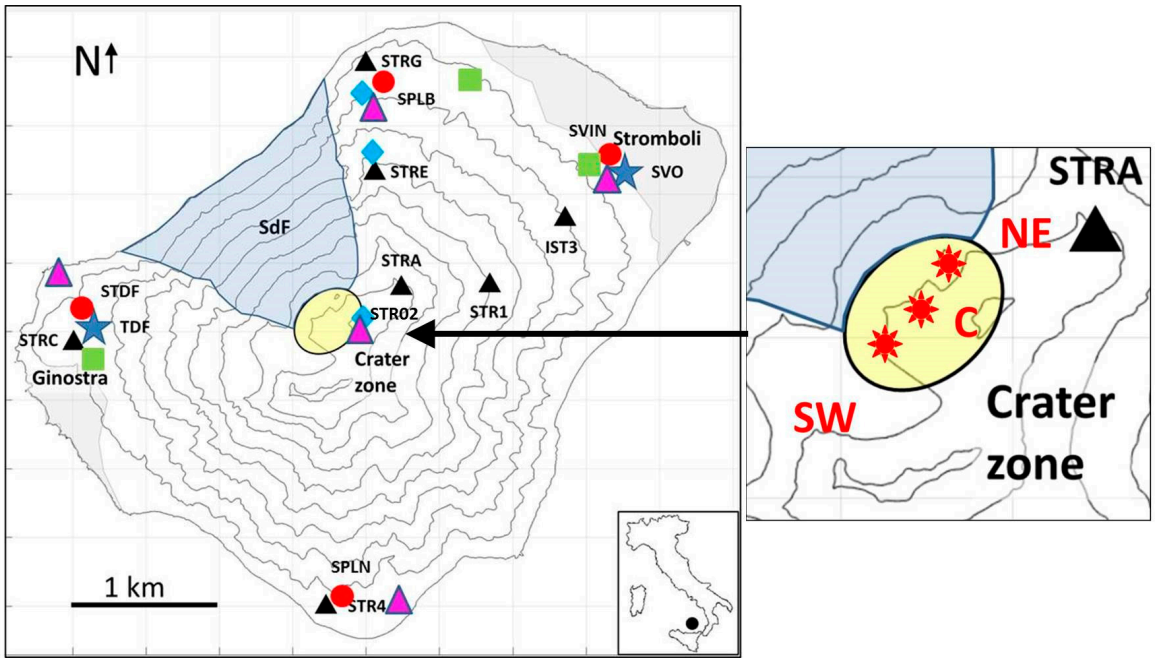

Figure 1. Left: Map of Stromboli island (and its location in southern Italy, inset) with the Stromboli and Ginostra villages, the "Sciara del Fuoco" depression (SdF), and the crater zone (yellow oval). The black triangles indicate the position of the seismic stations; the blue stars indicate the position of the strainmeters; the red circles are the GPS stations; the green squares are the tiltmeters; the blue diamonds are video-cameras, and the magenta triangles are the geochemical stations. Right: The crater zone with the main vent regions (red stars): Northeast (NE), central (C) and southwest (SW).

The persistent activity of Stromboli volcano was observed for several centuries [9–12], and its eruptive history was punctuated by effusive eruptions, major and paroxysmal explosions [1,11,13–15]. Major explosions are significantly larger than the ordinary explosions, and normally occur twice a year [16]. "Paroxysms" is used for even greater explosive eruptions that display an average occurrence of one event every 5–15 years [16]. The persistent explosive activity produces jets comprising a mixture of gas, ash and lapilli up to several tens of meters above the vents [17]. Major explosions result in heights of the ejecta up to several hundred meters above the vents [11], affecting the areas frequented by hikers visiting the volcano. Paroxysms generate eruptive columns rising a few kilometers above the vents [14–16,18–20] and can affect the villages of Ginostra and Stromboli located less than 2 km away from the vents (Figure 1).

The seismicity of Stromboli is dominated by the signals generated by the explosions that take place in the crater area, also called "explosion-quakes" that contain Very Long Period (VLP) events [1,21,22]. The VLP signals were fully investigated in [23] and resulted as generated by a seismic source, which was located ~250 m beneath and ~160 m northwest of the active vents (Figure 2d). The automatic monitoring of these signals [24], based on different location techniques such as radial semblance [25,26] and the moment tensor inversion [23,27], showed substantial stability of the source over several years, except for small variations recorded before and during the 2007 effusive eruption [24].

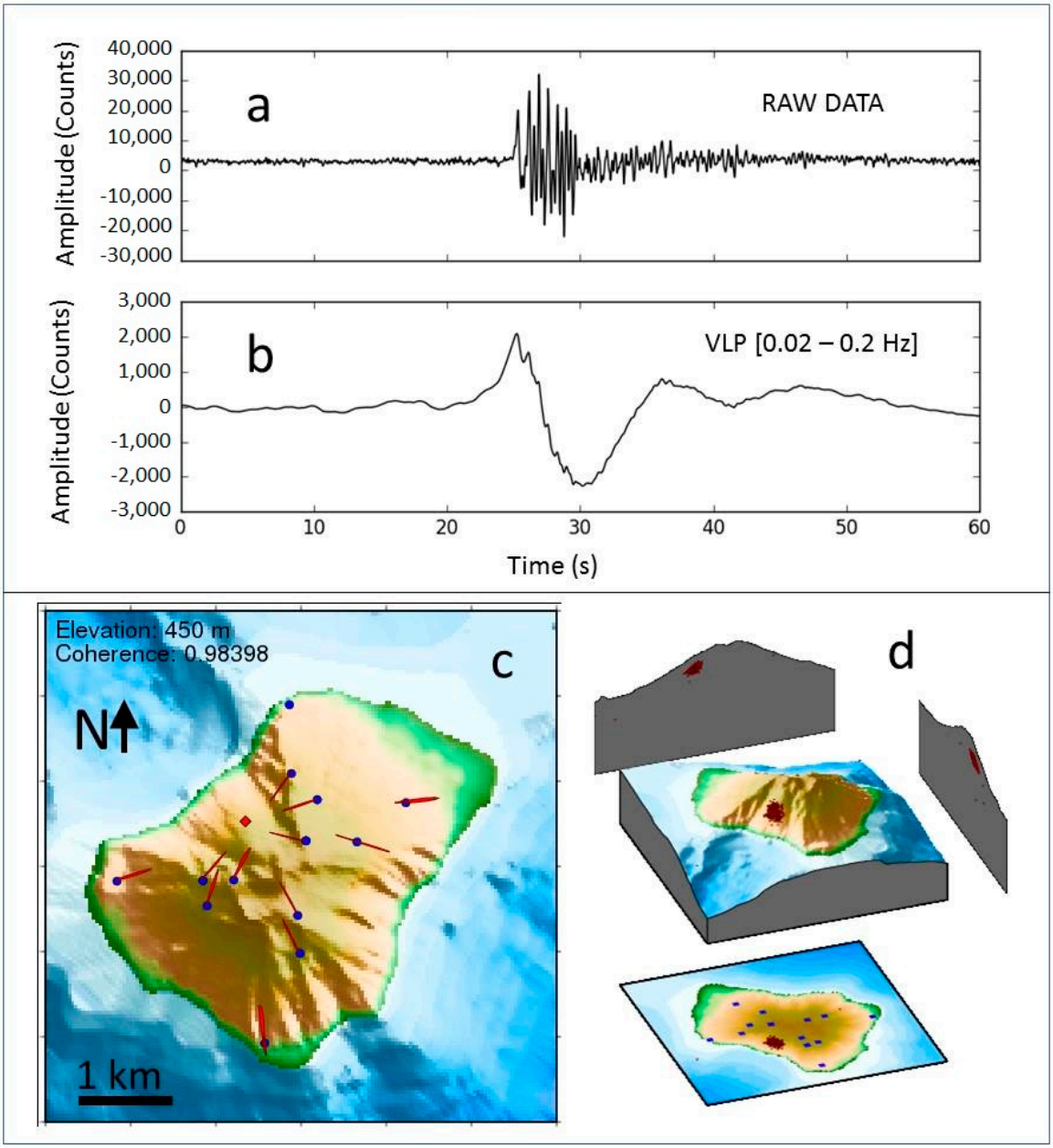

Figure 2. (**a**) Example of an explosion-quake recorded by STRA station (vertical component); (**b**) the same signal filtered in the VLP frequency band (0.02–0.2 Hz); (**c**) rose diagrams of the polarization direction of about 83,000 VLP events recorded in 2012, plotted on the map. The red diamond indicates the average source centroid, obtained from the polarization parameters, located 450m above sea level; the blue dots are the seismic stations. (**d**) The automatic locations of a subset of the VLP events recorded in 2012 carried out by the EOLO system (http://eolo.ov.ingv.it/eolo/). The subset consists of 1915 VLP events (in red) recorded by at least six stations (blue dots) with well-located hypocenters. The mean elevation of the VLP sources is about 400 m above sea level. The VLP sources retrieved by [23] are within the cloud of the VLP locations (in red).

Another characteristic of the Stromboli seismic wave-field is the volcanic tremor (Figure 2b), which forms a continuous background signal. It is interpreted as due to seismic waves generated in the shallow conduit [28]. Puffing, which occurs at the open vents (mainly at the central crater), also contributes to the volcanic tremor at Stromboli [29]. Other seismic signals typically recorded at Stromboli are due to landslides (Figure 2c), mostly occurring on the SdF. A significant increase of these

signals has been recognized as a short-term precursor of the two flank effusive eruptions in 2002–2003 and 2007 [1,30,31]. This observation highlighted the importance of the landslide seismic signals, which are constantly monitored [31,32].

Seismic signals due to explosions (VLP), landslides and volcanic tremor are routinely used to define the state of activity of Stromboli volcano [24] (Bollettini INGV—http://www.ct.ingv.it).

In the last decades, the eruptive history of Stromboli was dominated by three effusive flank eruptions, which occurred in 2002–2003 [13,33,34], in 2007 [1,5,35] and in 2014 [36–39], all within the SdF depression and associated with hazardous phenomena. At the end of 2002, the beginning of the flank eruption was associated with a landslide along the SdF that triggered a tsunami, which damaged the coast of the island [40–42]. During this eruption, which ended in July 2003, the monitoring system was improved by adding new geophysical and geochemical stations and developing a real-time processing system [22,43]. Before the end of the effusive eruption, on 5 April 2003 a paroxysmal explosion occurred [14,44], which destroyed some geophysical instruments installed in the summit area of the volcano and caused damage to the village of Ginostra (Figure 1) [45]. Another effusive eruption occurred on February–April 2007 [1,5] during which a paroxysmal explosion happened on 15 March 2007, anticipated by a strong step-like overpressure building up in the uppermost conduit [46,47]. During both the 2002–2003 and 2007 effusive eruptions the persistent summit explosive activity stopped or significantly decreased, as a result of magma drainage from the eruptive fissure [5,13,14]. After the 2007 effusive eruption, the persistent explosive summit activity of Stromboli resumed [48], but the eruptive activity changed, displaying several unusual overflows from the crater zone, a more than doubled number of major explosions, and absence of paroxysms [32,49,50]. The enhanced monitoring network allowed us to recognize that the effusive phases were preceded by a few weeks of increment of amplitude and occurrence rate of Very Long Period events (VLP) and associated number of explosions, which are related to the magma level within the shallow conduit [1,5,13,35]. A progressive increase of the volcanic tremor amplitude, accompanied by an anomalous occurrence of landslides within the SdF area a few hours before the beginning of the lava flow anticipated the effusive phases [1,31]. No important ground deformations were detected immediately before flank eruptions, but GPS and tilt measurements revealed two episodes of pure intrusion in 1994–1995 and 2000, and a continuous deflation during the entire 2007 eruption [51]. Conversely, the ground-based synthetic aperture radar (GB-InSAR) showed a progressive shallow movement of the NE crater portion preceding the 2007 eruption and a bulging on the SdF before vent opening [52]. Anomalous sulphur content in the degassing plume was recorded 2–3 days before the 5 April 2003 paroxysm [53] revealing the rising up of a gas-rich magma pocket in the uppermost conduit. SO_2 flux from the plume and CO_2 flux from the ground showed a marked increase during the 2007 eruption, when drainage of lava along the SdF caused the emptying of the upper part of the magma column and favoured the rise of a gas-rich magma batch [35].

The last effusive phase, which occurred in August–November 2014 [36,37], was preceded by overflows and increased Strombolian activity [39], and followed by a low eruptive activity period lasted until mid-2017, when a reawakening phase began. A more intense explosive activity started in May 2017, continued in the following months and led the Italian Civil Protection Department to decree the "attention" alert level (yellow code) on 7 December 2017, based mainly on seismic, thermal video-camera and geochemical observations that indicated a rise in magma level inside the upper conduits. An important characteristic of the reawakening phase was the increasing number of major explosions, which drove the crater area at risk. Nine major explosions occurred from July 2017 to August 2018 that, fortunately, did not produce damage. Major explosions are a typical hazard of Stromboli [11,16] because they can affect the summit area frequented by hikers. In response to this type of volcanic hazard, in 2006, the Italian Civil Protection Department set up shelters in the summit area of the volcano in order to mitigate the risk that hikers could be hit by ballistics [54]. Obviously, the use of these shelters would greatly benefit from a possible warning to be issued even a short time before a major explosion. Different volcanic events worldwide, such as the Ontake 2014 disaster [55],

have shown that even a few seconds of warning could significantly reduce the number of fatalities from small explosions.

In this paper, we analyze the recent reawakening phase of Stromboli (2017–2018), which was recorded by the INGV multidisciplinary networks, investigating the eruptive mechanism of major explosions. We select the well-recorded major explosion occurred on 1 December 2017, as a case study, and investigate the possibility of implementing a timely alarm method, based on multiple sensor recordings, in particular on seismic and strainmeter precursory signals.

2. Materials and Methods

In order to analyze the state of activity of Stromboli volcano in the period 2017–2018, we considered the data of the INGV video-camera, seismic, deformation, and CO_2 soil flux monitoring systems.

The ground-based remote sensing monitoring of explosive activity is performed by the thermal and visible video-cameras comprising the network installed by the INGV-Osservatorio Etneo (INGV-OE) on the volcano, having a capture rate of 0.5–2.0 images per second. The fixed camera network includes thermal infrared (~8–14 μm) and visible (400–700 nm) cameras located at 400 m elevation on the NE flank of the SdF, and at "Il Pizzo Sopra la Fossa", 890 m a.s.l., and ~250 m from the craters (Figure 1). To obtain a description of the eruptive activity, the total number of explosive events each day of cloud-free observation was manually counted and reported as an integer average hour value. On average, 5–9% of the days were affected by clouds and/or by system failure. In such cases, data are lacking [56].

In the period subject of this work, the seismic network included seven seismic stations (Figure 1). In the past, there were 14 stations [22] deployed by INGV-Osservatorio Vesuviano (INGV-OV), but from 2013 their number decreased because some sites became inaccessible both by land and by helicopter. The seismic stations are equipped with Guralp CMG 40T (60 s–50 Hz) velocimeters and Gilda data logger [57]. In 2006 two Sacks-Evertson borehole strainmeters [58,59] were added to the Stromboli geophysical network.

Ground deformation monitoring at Stromboli is mainly based on tilt and GPS data. Tilt is continuously monitored by using borehole stations (2.5–3.5 m deep), with AGI 722 sensors [60]. Since 2011, a deep (−27 m below ground level) station, equipped with AGI Lily tiltmeter, is operating at Timpone del Fuoco (TDF) [61]. About GPS measurements, INGV-OE manages a CGPS (Continuous Global Positioning System) network on Stromboli. Currently, four stations allow us to perform continuous monitoring of the ground deformations in real time. These CGPS stations are controlled from the master station at INGV-OE [62,63]. The stations (Figure 1) are: Punta Lena (SPLN), Punta Labronzo (SPLB), San Vincenzo (SVIN) and Timpone del Fuoco (STDF). A double processing strategy is applied to the data of this network: A 1 Hz real time processing [62] using RTD software [64], and a more precise 24 h/day sessions processing using GAMIT software [62,65]. In this work, only the high precision data obtained from the GAMIT software are shown.

The CO_2 flux emitted from the soil at "Il Pizzo Sopra la Fossa" (STR02) in the crater zone (Figure 1) is continuously monitored on an hourly basis [38] using accumulation-chamber equipment (West Systems, Pontedera (PI), Italy) [66]. The measured data are transmitted to the COA Civil Protection volcano observatory at Stromboli via a wide local area network (W-LAN) and also to the INGV-Palermo geochemical monitoring center via a virtual private network link.

3. Results

We describe here the results of the analysis of the most significant parameters monitored at Stromboli in the period May 2017–June 2018. These include the number of VLP events per hour associated with the explosions, the amplitude of the explosion-quakes, the amplitude of the volcanic tremor, the number of explosions detected by the video-cameras, the deformation of the edifice (tilt and length of GPS baselines), CO_2 flux and number of landslides occurred in the SdF. Plots of the time series of these parameters are reported in Figure 3 and are briefly described below.

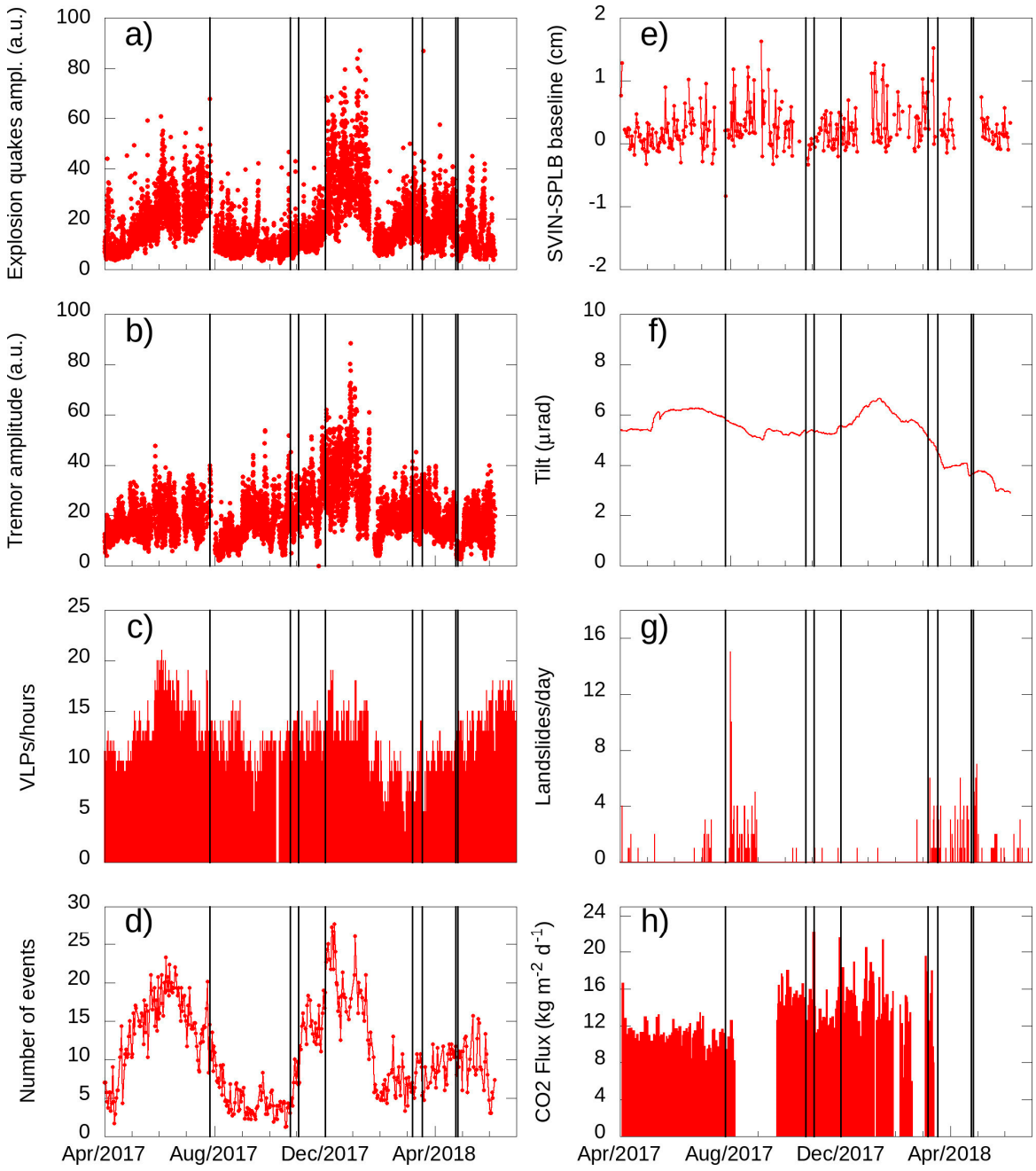

Figure 3. Variations of several monitoring parameters occurred between 1 April 2017 and 6 June 2018. The major explosions are marked in each graph by black vertical lines. (**a**) Amplitude of the explosion-quakes. (**b**) Volcanic tremor amplitude. (**c**) VLP hourly rate. (**d**) Explosion counting carried out using the INGV-OE video-camera network. We estimate a 10% error on the explosion counting. (**e**) GPS baseline length variations between SVIN and SPLB. (**f**) Tilt recorded at Timpone del Fuoco (TDF). The N275°E component is direct toward the summit area, and a positive signal variation means crater up. (**g**) Daily rate of landslides. (**h**) Summit soil CO_2 degassing at STR02 station.

For the analysis of seismic time series, we chose the data recorded by STRA station (Figure 1) that is close to the crater zone, in order to show the trend of the explosion-quake amplitude, the volcanic tremor amplitude and the VLP hourly rate. The amplitude of the explosion-quakes (Figure 3a) is controlled by the eruption jet. It is higher when the explosion produces a well-collimated jet of gases and pyroclastic fragments and high amplitude air waves [28].

The volcanic tremor recorded at Stromboli (Figure 3b) is interpreted as the result of the oscillation of the gas bubbles ascending in the magma conduit [28]. Also, puffing and spattering, which occur at the vents, can contribute to the tremor amplitude, as mentioned above [29]. Therefore, an increase of the tremor amplitude typically indicates a greater excitation of the conduit by the gas bubbles that move within the magma, and an increased puffing and spattering activity.

The VLP signals are intrinsically linked to the explosive source process. Therefore, the VLP occurrence rate (Figure 3c) gives us a direct measure of the explosion rate. This parameter shows a good agreement with the explosion counting carried out by using the video-camera images (Figure 3c,d), especially when the explosion-quakes amplitude (Figure 4a) is high.

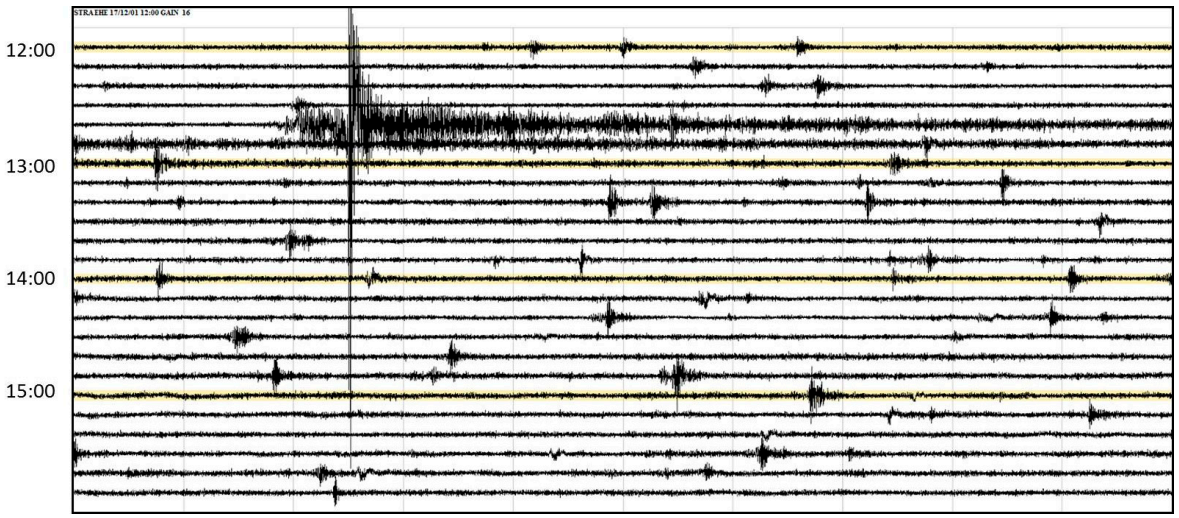

Figure 4. The major explosion occurred on 1 December 2017 at 12:42:30 UTC and the background explosive seismicity of Stromboli volcano due to the ordinary explosions (STRA east-west component). Time ranges from 12:00 to 16:00 UTC. The signal amplitude is expressed in counts. The distance between the two lines is the equivalent to 2048 counts.

The video-camera continuous recordings allow us to monitor the explosive activity and puffing and spattering activity. In Figure 3d, the image analysis of the INGV-OE permanent video-cameras is shown in terms of the total number of explosions per hour. The explosions occurred within the crater terrace from all the active vents are manually counted, and displayed as an integer.

The geodetic measurements are able to monitor ground deformations associated with magmatic processes at Stromboli [63]. Due to problems to the STDF station, we can show here only the baseline length variations between SVIN and SPLB stations (Figure 3e). Moreover, Figure 3f shows the data of the N275° component of the TDF tiltmeter that is directed towards the summit crater area.

The occurrence of landslide seismic signals is reported in Figure 3g. As already mentioned, the landslides were precursors of the recent effusive phases due to the opening of fractures on the SdF slope. For this reason, their occurrence rate is a significant parameter for the definition of the state of activity of the Stromboli volcano.

The geochemical monitoring, shown in Figure 3h, is aimed at evaluating the degassing degree on the summit area of Stromboli [38] and consists of the continuous CO_2 soil flux measurements by the STR02 station in the crater zone (Figure 1).

Between May 2017 and June 2018, eight major explosions were recorded, marked by black vertical lines in Figure 3. A further major explosion occurred on 18 August 2018 (not shown in Figure 3).

In Figure 3 the seismological parameters (explosion-quake amplitude, tremor amplitude and VLP hourly rate, Figure 3a–c) and the video-camera image analysis (Figure 3d), show two phases of increase of the explosive activity, from May to September 2017, and from October 2017 to January 2018, respectively. In the second period an effusive phase, due to a lava overflow from the NE crater, was

recorded on 15 December 2017. The soil CO_2 degassing (Figure 3h) is consistent with a general increase in eruptive activity. Actually, in the period from 2005 to 2015, we observed a slow continuous positive trend of CO_2 degassing [38] that culminated in the 2017–2018 with a strong abrupt increase of CO_2 flux. During the whole period considered here, the daily rate of seismic signals associated with landslides (Figure 3g) on the SdF flank did not show any anomaly, as well as the geodetic signals (Figure 3e,f).

The definition of major explosions, which is anything but univocal, is beyond the scope of this work. On this topic there is an extensive scientific literature [11,16,45,67]. Here we consider as major explosions those explosive events that generate a seismic signal significantly larger, in terms of amplitude and/or duration, compared to the seismic signals due to the ordinary explosive activity. Figure 4 shows the four-hour seismogram, from 12:00 to 16:00 UTC, of the STRA station, east-west component, recorded on 1 December 2017, in order to show the seismic signature of a major explosion compared to the background seismicity.

From 26 July 2017 to 26 April 2018, eight major explosions occurred (in nine months). Each seismogram shows a precursory phase that preceded the amplitude peak associated with the explosion. In the following, we will refer to this signal, which is particularly evident in the 1 December 2017 explosion, as a precursory signal.

The thermal video-camera network allowed us to reconstruct the dynamics of the major explosions recorded in the period here considered (July 2017–April 2018) and to identify their eruptive source vents. In particular, the major explosion of 26 July 2017 (Figure 5a) was a sequence of at least three pulses ejected from the central (C) and southwest (SW) vent regions (Figure 1). The seismogram filtered in the VLP frequency band (0.02–0.2 Hz) confirms the presence of multiple pulses in the seismic signal (Figure 5a). The major explosions that took place on 23 October, 1 November and 1 December, 2017 (Figure 5b–d respectively), also originated in the central (C) and southwest (SW) vent regions. The VLP seismograms relating to these explosions highlight the dominance of the main pulse that characterized the seismic source associated with the explosive process. The images of the explosion occurred on 1 December 2017 (Figure 5d), unfortunately, are not suitable for an in-depth analysis due to problems related to weather conditions and poor visibility. Nevertheless, they allowed us to recognize the source of this eruptive event in the southwest (SW) region (as also confirmed by other video-camera and infrasound observations reported by Florence University reports (https://www.dst.unifi.it/) and, subsequently, activation of the central vent region. The major explosion of 7 March 2018 (Figure 5e) took place in the northeast vent region (NE). The VLP seismogram associated with this major explosion had a smaller amplitude than those previously mentioned. The major explosion that occurred on 18 March 2018 (Figure 5f) originated from the central vent region (C) and also activated the northeast vent region (NE). The events of 24 April (Figure 5g) and 26 (Figure 5h) 2018 occurred in the southwest (SW) and central (C) vent regions and in the northeast (NE) vent region, respectively.

Among the major explosions occurred between July 2017 and April 2018, only the 1 December 2017 episode (Figure 5d) was recorded by one Sacks-Evertson borehole volumetric strainmeters, as well as by seven seismic stations, one infrasonic sensor, and one tiltmeter, thanks to favorable operating conditions of the monitoring system. The INGV Stromboli monitoring stations are deployed on the steep slopes of the island, and sometimes have problems of maintenance due to difficult access to the sites, poor weather, or powerful activity making instrument maintenance hazardous to people. Moreover, the presence of ash, fog or clouds may reduce the visibility or may prevent the batteries from charging. This demonstrates the utility of the instrumental redundancy and the importance of multi-parametric monitoring. For the above reasons, in the period here considered, we cannot rely on a high number of working stations. Therefore, we chose the explosion of 1 December 2017 as a case study. This event took place around 12:42 UTC from a vent in the SW region and also activated the central vent region, as retrieved by the thermal camera image analysis.

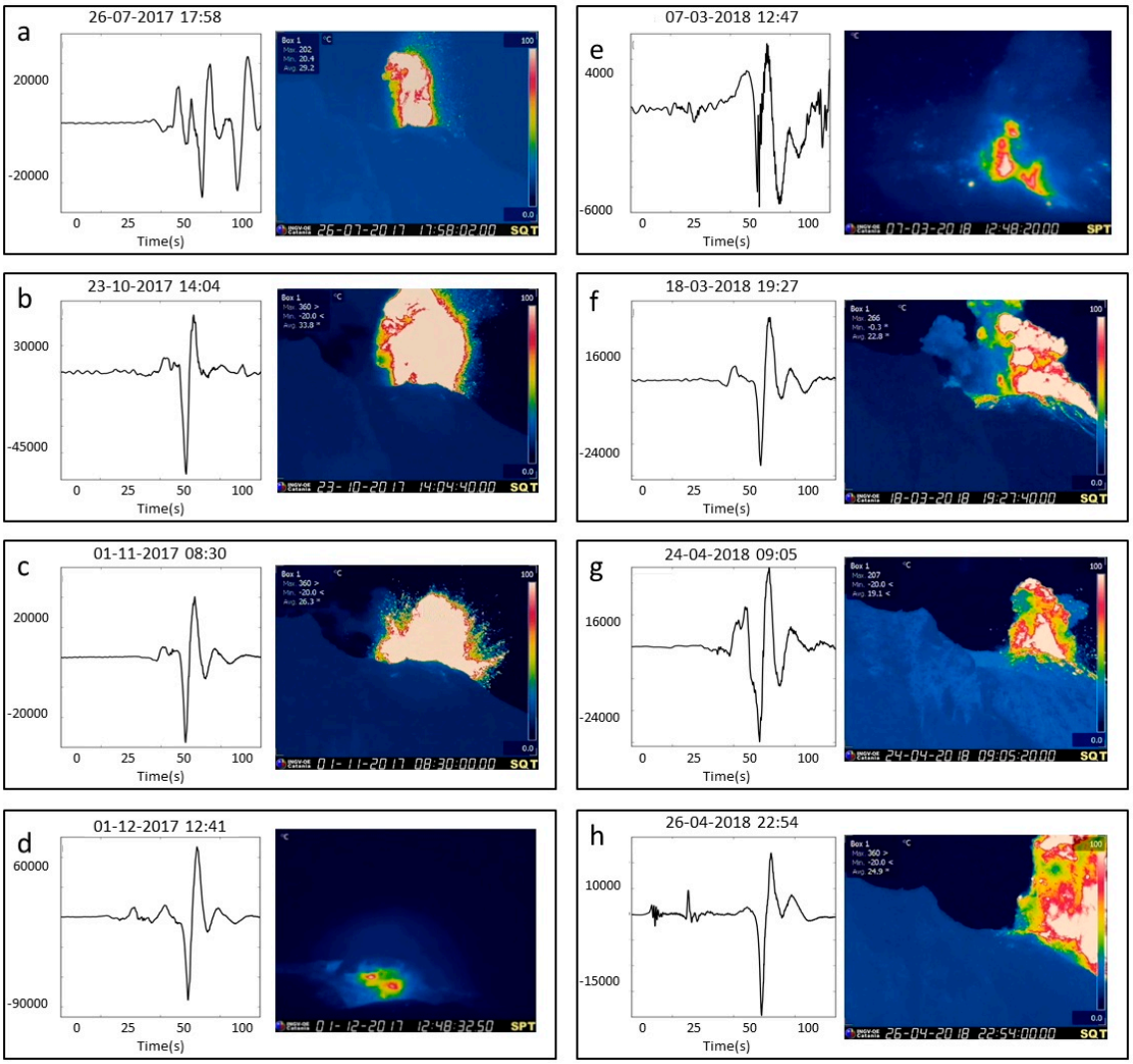

Figure 5. VLP seismograms and thermal images of the major explosions recorded by the thermal camera at 400 m elevation on the NE flank of the SdF (**a**–**c**,**f**–**h**) and by the thermal camera at "Il Pizzo Sopra la Fossa" (890 m a.s.l. and ~250 m from the craters) (**d**,**e**). The date and time of each episode is plotted in the format dd-mm-yyyy hh:mm at the top of each graph.

Figure 6 reports tilt changes recorded at TDF (Figure 1) during the 1 December 2017 explosion. A small permanent offset was recorded on the N275°E component after the explosion, as shown in Figure 6.

In Figure 7, we show the infrasound, seismic and strainmeter recordings of the major explosion on 1 December 2017. The beginning of the dilatometer signal associated with the major explosion, filtered in 0.0002–0.02 Hz frequency band is marked with a vertical dashed line. We remark that SVO strainmeter (Figure 1) recorded a variation several seconds before the other geophysical instruments detected the incoming major explosion signal. This feature will be exploited in the next section as part of the discussion dedicated to the proposal of a timely alarm method for the major explosions.

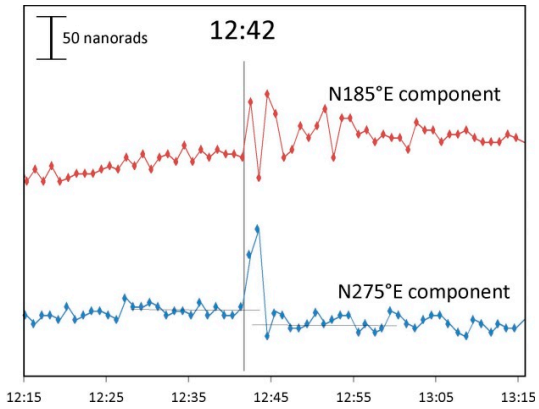

Figure 6. Tilt data recorded at the two components of TDF station between 12:15 and 13:15 UTC on 1 December 2017. Tilt sampling is one minute, and each value is the average of 8000 samples.

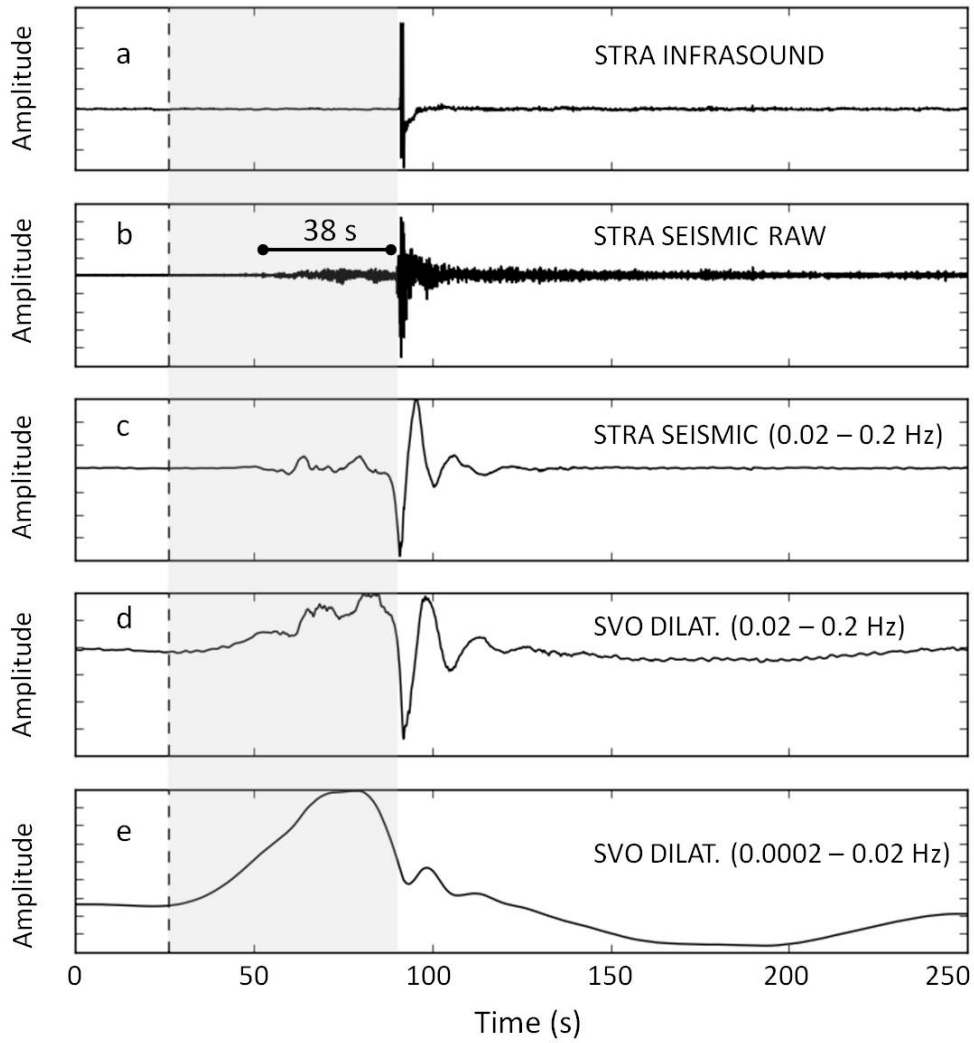

Figure 7. Recordings of the major explosion on 1 December 2017. The start time of the plot is 12:41:00.00 UTC. (**a**) Infrasonic signal (STRA, see Figure 1 for the location on the map); (**b**) raw seismic signal (STRA vertical component); (**c**) seismic signal filtered in the VLP band (0.02–0.2 Hz); (**d**) SVO strainmeter (see Figure 1 for the location on the map) filtered in the band 0.02–0.2 Hz; (**e**) SVO strainmeter (see Figure 1 for the location on the map) filtered in the 0.0002–0.02 Hz band. The grey area represents the lapse time between the initial variation detected by the strainmeter (**e**) and the start of the major explosion marked by the infrasonic signal (**a**).

The 1 December 2017 major explosion seismogram is characterized by a precursory phase of sustained oscillation lasting about 38 s (Figure 7b), with dominant frequency content around 1 Hz (Figure 8) and a VLP event (Figure 7c) with frequency content in the range 0.02–0.2 Hz (Figure 8).

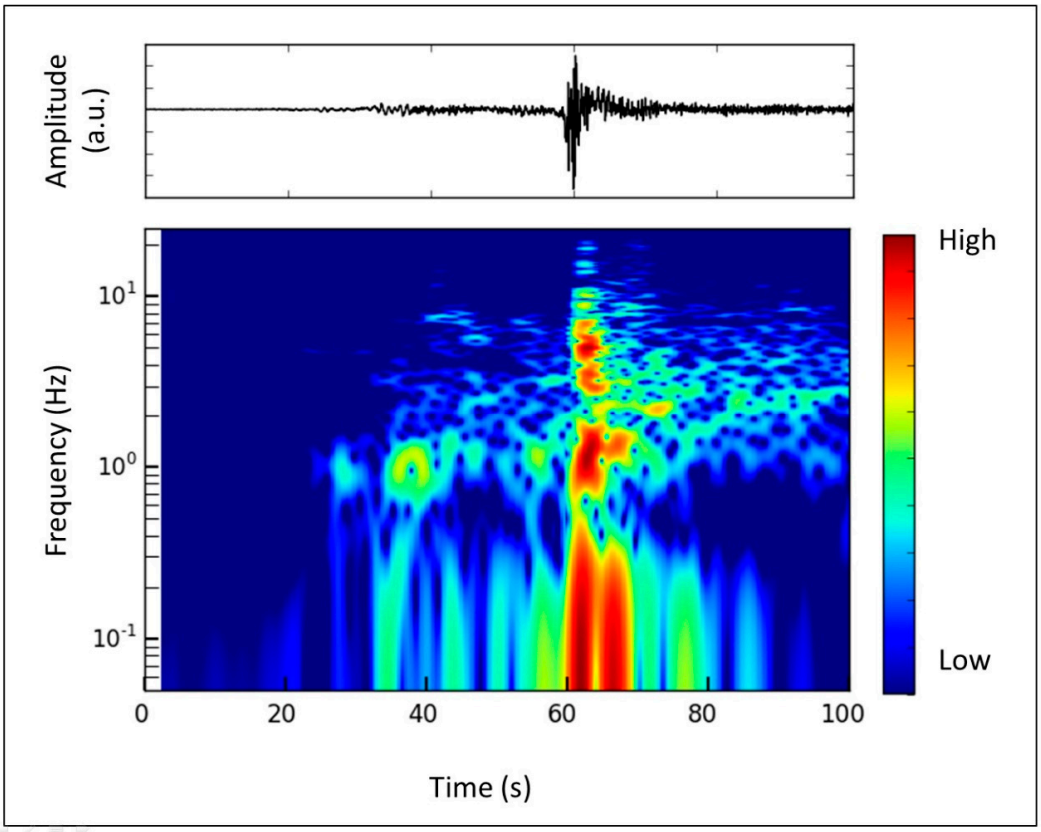

Figure 8. Seismogram (above) and spectrogram (below) of the 1 December 2017 major explosion (STRA vertical component).

Thanks to the remarkable amplitude of the signal (Figure 4), the beginning of the precursory signal has been clearly recorded at all the available seismic stations. We estimated the delay between the arrival times at the different seismic stations by performing the cross-correlation analysis between the onset of the vertical components, filtered in a narrow band around 1 Hz. Thus, we used the retrieved arrival times to locate the precursory signal, adopting a probabilistic approach based on the method proposed by [68]. Furthermore, we located the VLP event of the explosion exploiting its characteristic radial polarization. We calculated the polarization of the VLP pulse at four stations with adequate quality of the three-component signal: These are STRA, STR1, STRE and STRC stations (Figure 1). The results are shown in Figure 9 where the precursory signal and VLP locations, red circle and red star respectively, are compared with the locations of the VLPs recorded in 2012 (gray star and gray diamond), also shown in Figure 2. We can see that the location of the VLP event of the major explosion on 1 December 2017 falls within the typical zone of the VLP source locations (Figure 2). The location of the precursory signal is shallower and it is close to the southwestern vent region, from which the explosion originated, as seen above.

The GPS base-line between SPLB and STDF stations (Figure 1), across the SdF slope, which is sensitive to periods of magmatic recharge, is not available. However, the data of the North–South (N–S) component of SPLB station (Figure 10), showed a small displacement along the northern direction from the end of 2016 and the beginning of 2017, in correspondence with the start of the 2017–2018 phase. This displacement is compatible with modest inflation of the edifice due to the uprising of

magmatic fluids along with the main NE-SW structural trend, as already observed by [60,63]. This framework could explain the increase in the eruptive activity discussed in this study.

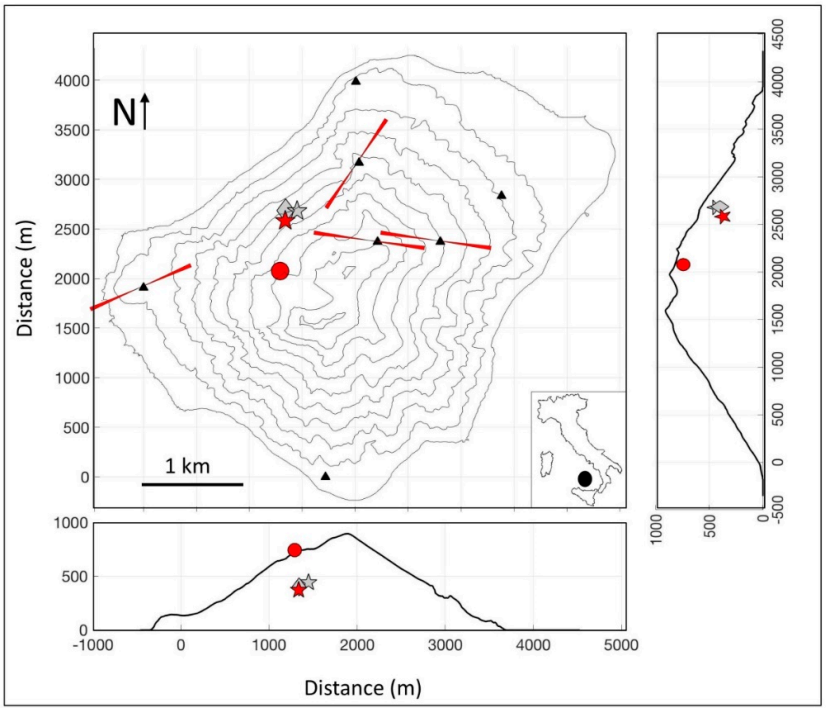

Figure 9. Locations of the precursory signal (red circle) and the VLP (red star, 311 m above sea level) of the 1 December 2017 major explosion, compared with the location of a dataset of 1915 VLP events mainly recorded in the first months of 2012. The gray star represents the centroid obtained from the polarization vectors of the VLPs recorded in 2012 (located 450 m above sea level). The gray diamond represents the area of maximum density of the localizations obtained with the analysis of semblances (386 events), about 400 m above sea level. The uncertainty on the precursory signal and VLP locations are about 100 m and 300 m in the position of the source, respectively.

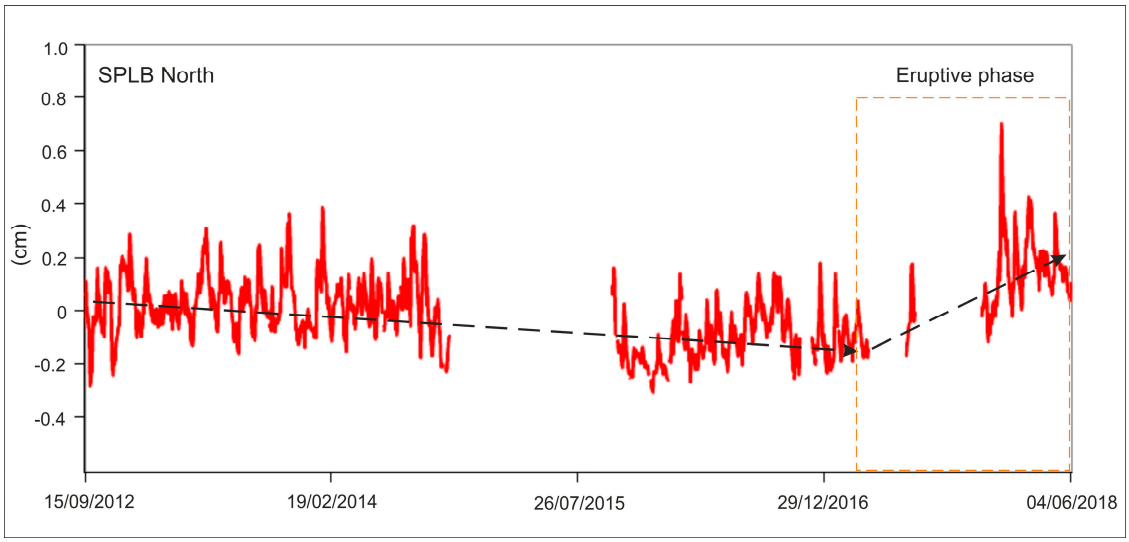

Figure 10. De-trended and filtered time series of the North−South component of the SPLB CGPS station. The second dashed black arrow indicates the increasing northward displacement of the station between 2016 and 2018. This displacement towards N (radial direction) is compatible with modest inflation of the volcano edifice.

4. Discussion

Thanks to its persistent explosive activity, Stromboli is a natural laboratory where pioneering studies on explosive eruptions and volcano monitoring have been conducted. After the tsunami that occurred on 30 December 2002 [40] and the paroxysmal explosions on 5 April 2003 [14], and 15 March 2007 [47], the potential social impact of the eruptive activity of Stromboli became evident to the scientific community and to the civil protection authorities. For this reason, many scientific studies and actions devoted to volcanic risk mitigation have been promoted in the following years. About fifteen years of geophysical and geochemical observations allowed the scientific community to highlight variations in the eruptive activity that prelude the beginning of the effusive phases [1,5,24,37,39]. Also in the period considered in the present paper, at the beginning of December 2017, the analyses of seismic, video-camera, geochemical, infrasonic and geodetic data allowed us to highlight a rise of the magma level in the conduits and to issue a warning, which leads the civil protection authorities to raise the alert code from green to yellow on 7 December 2017. Eight days later, on 15 December 2017, a small lava overflow occurred from the northeast crater (NE in Figure 1). Consistently with the lava overflow, the landslide rate did not show any significant anomaly, which is a short-term precursor of flank effusive phases linked to the opening of fractures on the SdF slope.

The video-camera, geophysical, and geochemical observations during the 2017–2018 eruptive phase gave us insights on the eruptive dynamics of Stromboli in this time interval. Between April 2017 and June 2018, the soil CO_2 flux measurements in the crater area showed a strong increase, characterized by a sharp input that confirmed the progressive growth observed in the last years [38,69], suggesting a fluid overpressure inside the volcanic edifice. This is associated with the increase of the volcanic tremor amplitude, of the VLP occurrence rate and of the increase in explosive activity at the crater area recorded by the video-camera images. All these signals indicate a greater formation and transport of gas slugs towards the eruptive vents, following a new volatile-rich magma input in 2017–2018.

The resumption of major explosions characterized the period covered by this work. The major explosions can occur for two main reasons: (i) Because a new input of gas-rich magma enters in the shallow conduit [15,67] or (ii) because of occasional blockages reducing the size of the summit vents and causing overpressure to grow below them [11]. While the movement of gas-rich magma at shallow level can be detected by the monitoring systems through the geophysical and geochemical observations (strain variations, thermal camera observations, SO_2 and CO_2 flux changes, deformations detected with GPS, tiltmeter, GBInSar measurements, etc.), the occasional blockages are unpredictable and occur with variable frequency, without any apparent correlation with other parameters related to the state of the volcanic activity. It is worth noting that the major explosions considered in this paper (Figure 3) occurred during phases of both high number of explosive events (>20 events/hour), when the level of magma is high within the shallow conduit [29,56], but also during phases with low or intermediate number of events (<10 events/hour). Furthermore, they originated from all the different vent regions (NE, C, and SW) as evidenced by the thermal camera measurements (Figure 5). This confirms that, even in the examined period, the major explosions can have different origins, either deep or shallow [11,45,67,70].

The case study of the 1 December 2017 recorded by different geophysical instruments, provides the opportunity of studying the mechanism of this type of events. In particular, we identified a seismic precursory signal and determined its source position, which is located at a small depth (740 m a.s.l.) below the SW vent region (Figure 9). When the seismic precursor is recorded, no correlated signal is distinguishable on infrasonic recordings, while the strainmeter data indicated a remarkable strain increase (Figure 7b,e). For this reason, we interpret the seismic precursor phase as related to the magma input inside the conduit below the SdF and not to degassing processes. The position of the seismic precursor source suggests that it is due to the oscillation, before the start of the major explosion, of a very shallow conduit in the SW vent region connected to the crack-like structure below the SdF. When the major explosion started, the crack collapsed, and the VLP event (Figure 7c) began. The jet of

the explosion produced the amplitude peak of the seismic signal and the high amplitude transient of the infrasonic signal. Consistently with these observations, a small permanent tilt at the TDF station (Figure 6), detected on N275°E component (ca. 15 nanorads), suggested a summit area contraction (deflation) during and after the explosive process.

The occurrence of the seismic precursory phase, lasting about 38 s, and the signal of the SVO strainmeter, which detected a strain change related to the major explosion even before the seismic stations recorded the precursory signal, suggest a possible implementation of a timely alarm system for future major explosions, similar to that of 1 December 2017.

We tested an automatic algorithm based on the Short-Term Averaging/Long-Term Averaging (STA/LTA) trigger method, appropriately tuned, on the strainmeter (Figure 11) and seismic data of 1 December 2017. We used "ObsPy" (http://www.obspy.org) seismic data analysis system [71], which includes routines for the calculation of STA/LTA [72,73]. We found that the most appropriate frequency band to highlight the beginning of the major explosion from the strainmeter signal is 0.004–0.02 Hz. We applied the STA/LTA algorithm over the band-pass filtered strainmeter signal. By choosing a short time window of 100 s and a long-time window of 800 s, we obtained the trigger shown in Figure 12 (orange line), without any false alarm over the signal of the whole day of 1 December 2017, shown in Figure 11. Moreover, we applied the algorithm on the seismic signal of the STRA and STRE stations, vertical components, filtered in the band that characterizes the precursory signal (0.6–1.0 Hz). We chose a short time window of 50 s, a long-time window of 400 s and an appropriate threshold to avoid false alarms by using the data of the test day of 1 December 2017.

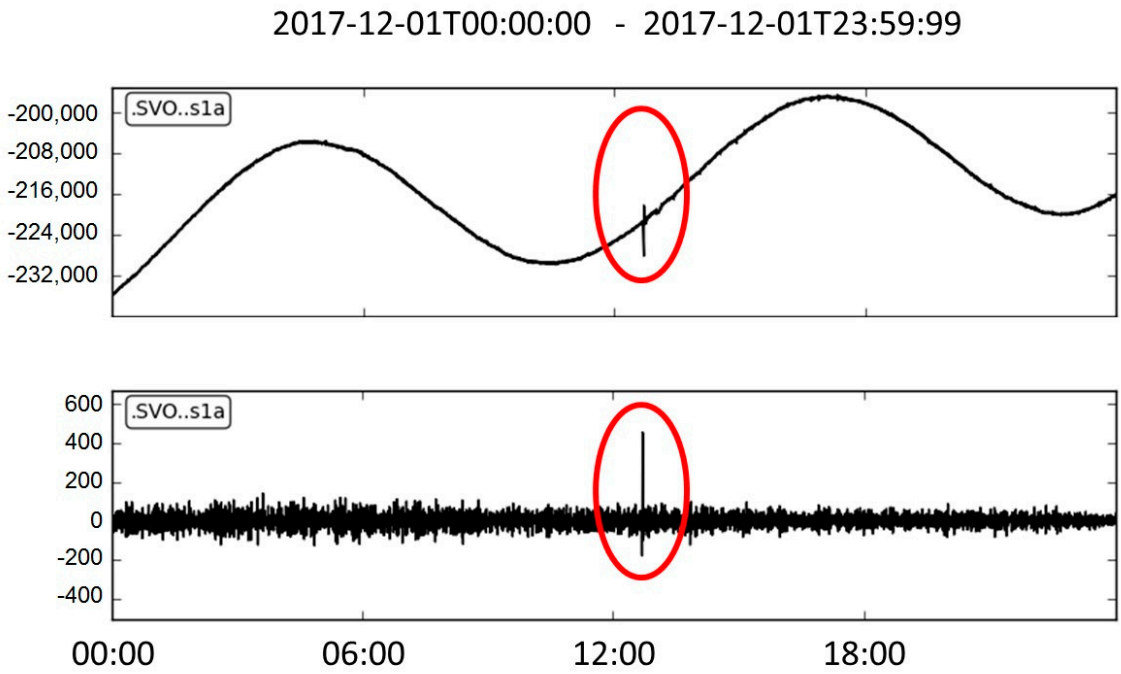

Figure 11. Raw SVO strainmeter (Figure 1) signal (upper panel) and band-pass (0.004–0.02 Hz) filtered SVO strainmeter signal (bottom panel). The red ellipses indicate the 1 December 2017, major explosion. The tidal component is evident on the upper unfiltered signal.

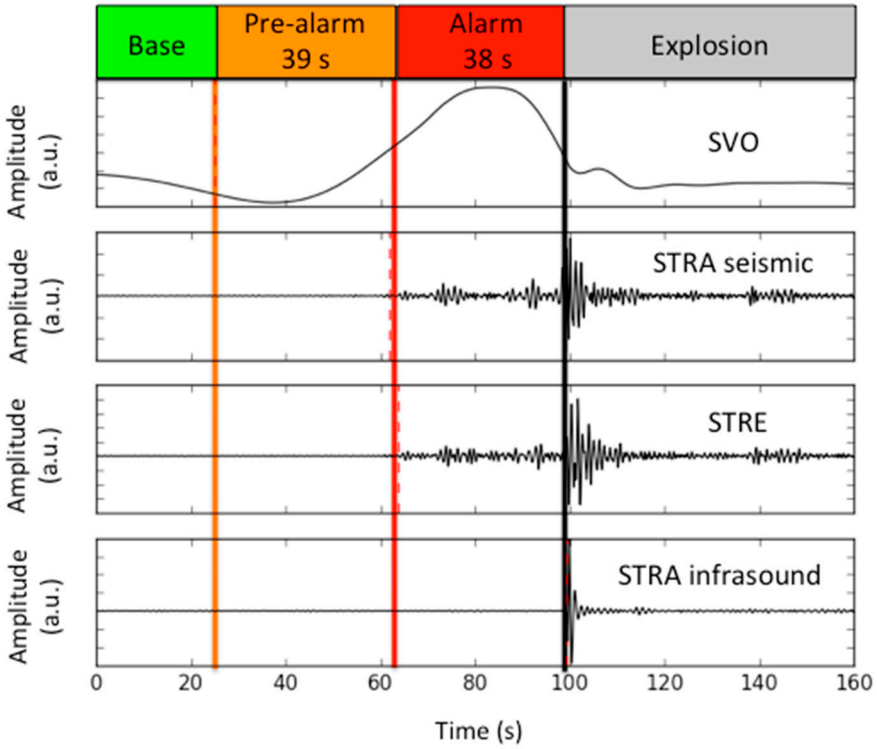

Figure 12. Outline of a proposal for a timely alarm system for the major explosions at Stromboli, based on strainmeter and seismic data. The vertical orange line marks the trigger of the Ultra Long Period signal, detected by the SVO borehole strainmeter 77 s before the potential impact of the explosion on the crater area, frequented by tourists. The red line marks the trigger of the seismic stations that recorded the precursory signal, about 38 s before the onset of the explosive phenomenon that is highlighted by the infrasound signal trigger (black line).

Our proposal for a timely alarm test for major explosion takes into account a pre-alarm, marked by the detection of the strainmeter signal anomaly (orange line in Figure 12), which in the case of 1 December 2017 occurred 77 s before the explosive activity could impact the summit area of Stromboli. The confirmation of the detection of an incoming major explosion was marked by the trigger of the precursory signal at least in two seismic station signals (red line in Figure 12). The occurrence of the explosive activity potentially able to impact the area visited by tourists is highlighted by the trigger of the infrasonic phase (black line in Figure 12).

This method was tested only on the major explosion of 1 December 2017. After being tested on a sufficient number of future major explosions, this proposal could become a very useful routine in our observatory. In fact, a timely received 77 or even 38 s in advance would allow people on the top of the volcano to safely reach the shelters, located near the explosive activity observation area, in time and avoid any damage.

5. Conclusions

The integration of in situ and ground-based remote sensing measurements allowed us to recognize the 2017–2018 reawakening phase of Stromboli volcano and to follow its evolution over time. This phase led to the raising of the alert level on the island from "green" (base level) to "yellow" (attention level) on 7 December 2017, and was characterized by a small lava overflow from the NE crater rim on 15 December 2017 and by a high occurrence rate of major explosions (8 events in 9 months, between 26 July 2017 and 26 April 2018). The geophysical, video-camera and geochemical observations (Figure 3) indicate that the phase of increase of eruptive activity is consistent with an increase of volatile-rich magma feeding the system.

The resumption of the major explosions (Figure 5), fortunately without damage, gave us the opportunity to gain new insights into the mechanism of this process, which is the main hazard for tourists visiting the crater zone. The major explosions recorded in the 2017–2018 period involved different vents of the crater zone and occurred both when the eruptive activity was high and when was low, indicating that their origin can be either deep or shallow.

The analysis of the well-recorded major explosion of 1 December 2017 (Figures 7 and 9) allowed us to highlight that the source of the VLP component of this major explosion falls within the same volume where the VLP locations of the 2012 ordinary activity are clustered (Figures 2 and 9) suggesting a shallow storage whose depth is persistent over time. For this explosion, we identified and located a seismic precursor, which consists of a sustained oscillation lasting for several seconds (Figure 9).

Furthermore, the strainmeter and seismic precursors of the 1 December 2017 major explosion provided the opportunity to propose an automatic alarm criterion for this type of explosions, that could give a timely alarm 77 or even 38 s in advance and would allow people on the top of the volcano to safely reach the shelters, located near the explosive activity observation area, and avoid any damage.

Author Contributions: Conceptualization, F.G., S.C., L.D. and G.M.; geodesy, A.B., V.B., S.G., M.M. (Mario Mattia); Seismology, F.G., S.A., F.B., T.C., L.D., W.D.C., A.M.E., M.M. (Marcello Martini), M.O., R.P., E.P., G.S., A.T.; Geochemistry, S.I., A.P., F.V.; Video-cameras, A.C., S.C.; Seismic and strainmeter data analysis, F.G., L.D., G.M., P.R., B.D.L.

Funding: This research received no external funding.

Acknowledgments: We wish to thank all the many colleagues who have contributed to the monitoring effort on Stromboli. We are particularly indebted to the INGV technical staff who ensure the regular working of the multidisciplinary monitoring networks. This work benefited of the EU (DG ECHO) Project EVE n. 826292 and of the project INGV-FISR-2017 "Sale Operative Integrate e Reti di Monitoraggio del futuro: l'INGV 2.0". The data used in this study were provided by the Istituto Nazionale di Geofisica e Vulcanologia (Osservatorio Vesuviano, Osservatorio Etneo and Sezione di Palermo).

Conflicts of Interest: The authors declare no conflict of interest.

References

1. Martini, M.; Giudicepietro, F.; D'Auria, L.; Esposito, A.M.; Caputo, T.; Curciotti, R.; De Cesare, W.; Orazi, M.; Scarpato, G.; Caputo, A.; et al. Seismological monitoring of the February 2007 effusive eruption of the Stromboli volcano. *Ann. Geophys.* **2007**, *50*, 775–788. [CrossRef]
2. Allard, P.; Carbonnelle, J.; Mètrich, N.; Loyer, H.; Zettwog, P. Sulphur output and magma degassing of Stromboli volcano. *Nature* **1994**, *368*, 326–330. [CrossRef]
3. Burton, M.; Allard, P.; Murè, F.; La Spina, A. Magmatic gas composition reveals the source depth of slug-driven Strombolian explosive activity. *Science* **2007**, *317*, 227–230. [CrossRef] [PubMed]
4. Burton, M.R.; Salerno, G.G.; D'Auria, L.; Caltabiano, T.; Murè, F.; Maugeri, R. SO2 flux monitoring at Stromboli with the new permanent INGV SO2 camera system: A comparison with the FLAME network and seismological data. *J. Volcanol. Geotherm. Res.* **2015**, *300*, 95–102. [CrossRef]
5. Calvari, S.; Lodato, L.; Steffke, A.; Cristaldi, A.; Harris, A.J.L.; Spampinato, L.; Boschi, E. The 2007 Stromboli eruption: Event chronology and effusion rates using thermal infrared data. *J. Geophys. Res.* **2010**, *115*, B04201. [CrossRef]
6. Tioukov, V.; Alexandrov, A.; Bozza, C.; Consiglio, L.; D'Ambrosio, N.; De Lellis, G.; De Sio, C.; Giudicepietro, F.; Macedonio, G.; Miyamoto, S.; et al. First muography of Stromboli volcano. *Sci. Rep.* **2019**, *9*, 6695. [CrossRef] [PubMed]
7. Bertagnini, A.; Landi, P. The Secche di Lazzaro pyroclastics of Stromboli volcano: A phreatomagmatic eruption related to the Sciara del Fuoco sector collapse. *Bull. Volcanol.* **1996**, *58*, 239–245. [CrossRef]
8. Tibaldi, A. Multiple sector collapses at Stromboli volcano, Italy: How they work. *Bull. Volcanol.* **2001**, *63*, 112–125. [CrossRef]
9. Mercalli, G. Natura nelle eruzioni dello Stromboli ed in generale dell'attività sismo-vulcanica delle isole Eolie. *Atti Soc. Ital. Sci. Nat.* **1881**, *24*, 105–134.
10. Rosi, M.; Bertagnini, A.; Landi, P. Onset of the persistent activity at Stromboli volcano (Italy). *Bull. Volcanol.* **2000**, *62*, 294–300. [CrossRef]

11. Calvari, S.; Büttner, R.; Cristaldi, A.; Dellino, P.; Giudicepietro, F.; Orazi, M.; Peluso, R.; Spampinato, L.; Zimanowski, B.; Boschi, E. The 7 September 2008 Vulcanian explosion at Stromboli volcano: Multiparametric characterization of the event and quantification of the ejecta. *J. Geophys. Res.* **2012**, *117*, B05201. [CrossRef]
12. Leduc, L.; Gurioli, L.; Harris, A.; Colò, L.; Rose-Koga, E.F. Types and mechanisms of strombolian explosions: Characterization of a gas-dominated explosion at Stromboli. *Bull. Volcanol.* **2015**, *77*, 8. [CrossRef]
13. Calvari, S.; Spampinato, L.; Lodato, L.; Harris, A.J.L.; Patrick, M.R.; Dehn, J.; Burton, M.R.; Andronico, D. Chronology and complex volcanic processes during the 2002-2003 flank eruption at Stromboli volcano (Italy) reconstructed from direct observations and surveys with a handheld thermal camera. *J. Geophys. Res.* **2005**, *110*, B02201. [CrossRef]
14. Calvari, S.; Spampinato, L.; Lodato, L. The 5 April 2003 vulcanian paroxysmal explosion at Stromboli volcano (Italy) from field observations and thermal data. *J. Volcanol. Geotherm. Res.* **2006**, *149*, 160–175. [CrossRef]
15. Pistolesi, M.; Delle Donne, D.; Pioli, L.; Rosi, M.; Ripepe, M. The 15 March 2007 explosive crisis at Stromboli volcano, Italy: Assessing physical parameters through a multidisciplinary approach. *J. Geophys. Res.* **2011**, *116*, B12. [CrossRef]
16. Barberi, F.; Rosi, M.; Sodi, A. Volcanic hazard assessment at Stromboli based on review of historical data. *Acta Vulcanol.* **1993**, *3*, 173–187.
17. Patrick, M.R.; Harris, A.J.L.; Ripepe, M.; Dehn, J.; Rothery, D.A.; Calvari, S. Strombolian explosive styles and source conditions: Insights from thermal (FLIR) video. *Bull. Volcanol.* **2007**, *69*, 679–784. [CrossRef]
18. Pistolesi, M.; Rosi, M.; Pioli, L.; Renzulli, A.; Bertagnini, A.; Andronico, D. The paroxysmal event and its deposits. In *The Stromboli Volcano: An Integrated Study of the 2002–2003 Eruption*; Calvari, S., Inguaggiato, S., Puglisi, G., Ripepe, M., Rosi, M., Eds.; Number 182 in Geophysical Monograph Series; AGU: Washington, DC, USA, 2008; pp. 317–329.
19. Dellino, P.; Dioguardi, F.; Zimanowski, B.; Büttner, R.; Mele, D.; La Volpe, L.; Sulpizio, R.; Doronzo, D.M.; Sonder, I.; Bonasia, R.; et al. Conduit flow experiments help constraining the regime of explosive eruptions. *J. Geophys. Res.* **2010**, *115*, B04204. [CrossRef]
20. Bertagnini, A.; Di Roberto, A.; Pompilio, M. Paroxysmal activity at Stromboli: Lessons from the past. *Bull. Volcanol.* **2011**, *73*, 1229–1243. [CrossRef]
21. Neuberg, J.; Luckett, R.; Ripepe, M.; Braun, T. Highlights from a seismic broadband array on Stromboli volcano. *Geophys. Res. Lett.* **1994**, *21*, 749–752. [CrossRef]
22. De Cesare, W.; Orazi, M.; Peluso, R.; Scarpato, G.; Caputo, A.; D'Auria, L.; Giudicepietro, F.; Martini, M.; Buonocunto, C.; Capello, M.; et al. The Broadband Seismic Network of Stromboli Volcano, Italy. *Seismol. Res. Lett.* **2009**, *80*, 435–439. [CrossRef]
23. Chouet, B.; Dawson, P.; Ohminato, T.; Martini, M.; Saccorotti, G.; Giudicepietro, F.; De Luca, G.; Milana, G.; Scarpa, R. Source mechanisms of explosions at Stromboli Volcano, Italy, determined from moment-tensor inversion of very-long period data. *J. Geophys. Res.* **2003**, *108*. [CrossRef]
24. Giudicepietro, F.; D'Auria, L.; Martini, M.; Orazi, M.; Peluso, R.; De Cesare, W.; Scarpato, G. Changes in the VLP seismic source during the 2007 Stromboli eruption. *J. Volcanol. Geotherm. Res.* **2009**, *182*, 162–171. [CrossRef]
25. Chouet, B.; Saccorotti, G.; Dawson, P.; Martini, M.; Scarpa, R.; De Luca, G.; Milana, G.; Cattaneo, M. Broadband measurements of the sources of explosions at Stromboli Volcano, Italy. *Geophys. Res. Lett.* **1999**, *26*, 1937–1940. [CrossRef]
26. Kawakatsu, H.; Kaneshima, S.; Matsubayashi, H.; Ohminato, T.; Sudo, Y.; Tsutsui, T.; Uhira, K.; Yamasato, H.; Ito, H.; Legrand, D. Aso94: Aso seismic observation with broadband instruments. *J. Volcanol. Geotherm. Res.* **2000**, *101*, 129–154. [CrossRef]
27. Auger, E.; D'Auria, L.; Martini, M.; Chouet, B.; Dawson, P. Real-time monitoring and massive inversion of source parameters of very long period seismic signals: An application to Stromboli Volcano, Italy. *Geophys. Res. Lett.* **2006**, *33*, L04301. [CrossRef]
28. Chouet, B.; Saccorotti, G.; Martini, M.; Dawson, P.; De Luca, G.; Milana, G.; Scarpa, R. Source and path effects in the wavefields of tremor and explosions at Stromboli Volcano, Italy. *J. Geophys. Res.* **1997**, *102*, 15129–15150. [CrossRef]
29. Ripepe, M.; Gordeev, E. Gas bubble dynamics model for shallow volcanic tremor at Stromboli. *J. Geophys. Res. Solid Earth* **1999**, *104*, 10639–10654. [CrossRef]

30. Esposito, A.M.; Giudicepietro, F.; Scarpetta, S.; D'Auria, L.; Marinaro, M.; Martini, M. Automatic discrimination among landslide, explosion-quake, and microtremor seismic signals at Stromboli Volcano using neural networks. *BSSA* **2006**, *96*, 1230–1240. [CrossRef]
31. Esposito, A.M.; D'Auria, L.; Giudicepietro, F.; Peluso, R.; Martini, M. Automatic recognition of landslides based on neural network analysis of seismic signals: An Application to the monitoring of Stromboli Volcano (Southern Italy). *Pure Appl. Geophys.* **2013**, *170*, 1821–1832. [CrossRef]
32. Calvari, S.; Bonaccorso, A.; Madonia, P.; Neri, M.; Liuzzo, M.; Salerno, G.G.; Behncke, B.; Caltabiano, T.; Cristaldi, A.; Giuffrida, G.; et al. Major eruptive style changes induced by structural modifications of a shallow conduit system: The 2007-2012 Stromboli case. *Bull. Volcanol.* **2014**, *76*, 841. [CrossRef]
33. Brusca, L.; Inguaggiato, S.; Longo, M.; Madonia, P.; Maugeri, R. The 2002-2003 eruption of Stromboli (Italy): Evaluation of the volcanic activity by means of continuous monitoring of soil temperature, CO2 flux, and meteorological parameters. *Geochem. Geophys. Geosyst.* **2004**, *5*, Q12001. [CrossRef]
34. Carapezza, M.; Inguaggiato, S.; Brusca, L.; Longo, M. Geochemical precursors of the activity of an open-conduit volcano: The Stromboli 2002-2003 eruptive events. *Geophys. Res. Lett.* **2004**, *31*, L07620. [CrossRef]
35. Inguaggiato, S.; Vita, F.; Rouwet, D.; Bobrowski, N.; Morici, S.; Sollami, A. Geochemical evidence of the renewal of volcanic activity inferred from CO2 soil and SO2 plume fluxes: The 2007 Stromboli eruption (Italy). *Bull. Volcanol.* **2011**, *73*, 443–456. [CrossRef]
36. Rizzo, A.L.; Federico, C.; Inguaggiato, S.; Sollami, A.; Tantillo, M.; Vita, F.; Bellomo, S.; Longo, M.; Grassa, F.; Liuzzo, M. The 2014 effusive eruption at Stromboli volcano (Italy): Inferences from soil CO2 flux and 3He/4He ratio in thermal waters. *Geophys. Res. Lett.* **2015**, *42*, 2235–2243. [CrossRef]
37. Valade, S.; Lacanna, G.; Coppola, D.; Laiolo, M.; Pistolesi, M.; Donne, D.D.; Genco, R.; Marchetti, E.; Ulivieri, G.; Allocca, C.; et al. Tracking dynamics of magma migration in open-conduit systems. *Bull. Volcanol.* **2016**, *78*, 78. [CrossRef]
38. Inguaggiato, S.; Vita, F.; Cangemi, M.; Mazot, A.; Sollami, A.; Calderone, L.; Morici, S.; Paz, M.P.J. Stromboli volcanic activity variations inferred from observations of fluid geochemistry: 16 years of continuous monitoring of soil CO2 fluxes (2000–2015). *Chem. Geol.* **2017**, *469*, 69–84. [CrossRef]
39. Di Traglia, F.; Calvari, S.; D'Auria, L.; Nolesini, T.; Bonaccorso, A.; Fornaciai, A.; Esposito, A.; Cristaldi, A.; Favalli, M.; Casagli, N. The 2014 effusive eruption at Stromboli: New insights from in situ and remote-sensing measurements. *Remote Sens.* **2018**, *10*, 2035. [CrossRef]
40. Bonaccorso, A.; Calvari, S.; Garfì, G.; Lodato, L.; Patanè, D. Dynamics of the December 2002 flank failure and tsunami at Stromboli volcano inferred by volcanological and geophysical observations. *Geophys. Res. Lett.* **2003**, *30*, 1941. [CrossRef]
41. Tinti, S.; Pagnoni, G.; Zaniboni, F. The landslides and tsunamis of the 30th of December 2002 in Stromboli analysed through numerical simulations. *Bull. Volcanol.* **2006**, *68*, 462–479. [CrossRef]
42. Chiocci, F.L.; Romagnoli, C.; Tommasi, P.; Bosman, A. The Stromboli 2002 tsunamigenic submarine slide: Characteristics and possible failure mechanisms. *J. Geophys. Res.* **2008**, *113*. [CrossRef]
43. Bertolaso, G.; Bonaccorso, A.; Boschi, E. Scientific community and civil protection synergy during the Stromboli 2002-03 eruption. In *The Stromboli Volcano. An Integrated Study of the 2002–2003 Eruption*; Calvari, S., Inguaggiato, S., Puglisi, G., Ripepe, M., Rosi, M., Eds.; Geophysical Monograph Series; AGU: Washington, DC, USA, 2008; p. 387.
44. D'Auria, L.; Giudicepietro, F.; Martini, M.; Peluso, R. Seismological insight into the kinematics of the 5 April 2003 vulcanian explosion at Stromboli volcano (southern Italy). *Geophys. Res. Lett.* **2006**, *33*, L08308. [CrossRef]
45. Rosi, M.; Bertagnini, A.; Harris, A.J.L.; Pioli, L.; Pistolesi, M.; Ripepe, M. A case history of paroxysmal explosion at Stromboli: Timing and dynamics of the April 5, 2003 event. *Earth Planet. Sci. Lett.* **2006**, *243*, 594–606. [CrossRef]
46. Calvari, S.; Spampinato, L.; Bonaccorso, A.; Oppenheimer, C.; Rivalta, E.; Boschi, E. Lava effusion—A slow fuse for paroxysms at Stromboli volcano? *Earth Planet. Sci. Lett.* **2011**, *301*, 317–323. [CrossRef]
47. Bonaccorso, A.; Calvari, S.; Linde, A.; Sacks, S.; Boschi, E. Dynamics of the shallow plumbing system investigated from borehole strainmeters and cameras during the 15 March, 2007 Vulcanian paroxysm at Stromboli volcano. *Earth Planet. Sci. Lett.* **2012**, *357*, 249–256. [CrossRef]

48. Marotta, E.; Calvari, S.; Cristaldi, A.; D'Auria, L.; Di Vito, M.A.; Moretti, R.; Peluso, R.; Spampinato, L.; Boschi, E. Reactivation of Stromboli's summit craters at the end of the 2007 effusive eruption detected by thermal surveys and seismicity. *J. Geophys. Res. Solid Earth* **2015**, *120*, 7376–7395. [CrossRef]
49. Di Traglia, F.; Intrieri, E.; Nolesini, T.; Bardi, F.; Del Ventisette, C.; Ferrigno, F.; Frangioni, S.; Frodella, W.; Gigli, G.; Lotti, A.; et al. The ground-based InSAR monitoring system at Stromboli volcano: Linking changes in displacement rate and intensity of persistent volcanic activity. *Bull. Volcanol.* **2014**, *76*, 786. [CrossRef]
50. Di Traglia, F.; Battaglia, M.; Nolesini, T.; Lagomarsino, D.; Casagli, N. Shifts in the eruptive styles at Stromboli in 2010–2014 revealed by ground-based InSAR data. *Sci. Rep.* **2015**, *5*, 13569. [CrossRef]
51. Bonaccorso, A.; Gambino, S.; Mattia, M.; Guglielmino, F.; Puglisi, G.; Boschi, E. Insight on recent Stromboli eruption inferred from terrestrial and satellite ground deformation measurements. *J. Volcanol. Geotherm. Res.* **2009**, *182*, 172–181. [CrossRef]
52. Casagli, N.; Tibaldi, A.; Merri, A.; Del Ventisette, C.; Apuani, T.; Guerri, L.; Fortuny-Guash, J.; Tarchi, D. Deformation of Stromboli Volcano (Italy) during the 2007 eruption revealed by radar interferometry, numerical modelling and structural geological field data. *J. Volcanol. Geotherm. Res.* **2009**, *182*, 182–200. [CrossRef]
53. Aiuppa, A.; Federico, C. Anomalous magmatic degassing prior to the 5th April 2003 paroxysm on Stromboli. *Geophys. Res. Lett.* **2004**, *31*, L14607. [CrossRef]
54. Bertolaso, G.; De Bernardinis, B.; Bosi, V.; Cardaci, C.; Ciolli, S.; Colozza, R.; Cristiani, C.; Mangione, D.; Ricciardi, A.; Rosi, M.; et al. Civil protection preparedness and response to the 2007 eruptive crisis of Stromboli volcano, Italy. *J. Volcanol. Geotherm. Res.* **2009**, *182*, 269–277. [CrossRef]
55. Maeno, F.; Nakada, S.; Oikawa, T.; Yoshimoto, M.; Komori, J.; Ishizuka, Y.; Takeshita, Y.; Shimano, T.; Kaneko, T.; Nagai, M. Reconstruction of a phreatic eruption on 27 September 2014 at Ontake volcano, central Japan, based on proximal pyroclastic density current and fallout deposits. *Earth Planets Space* **2016**, *68*, 82. [CrossRef]
56. Calvari, S.; Intrieri, E.; Di Traglia, F.; Bonaccorso, A.; Casagli, N.; Cristaldi, A. Monitoring crater-wall collapse at active volcanoes: A study of the 12 January 2013 event at Stromboli. *Bull. Volcanol.* **2016**, *78*, 39. [CrossRef]
57. Orazi, M.; Martini, M.; Peluso, R. Data acquisition for volcano monitoring. *Eos Trans. Am. Geophys. Union* **2006**, *87*, 385–392. [CrossRef]
58. Sacks, I.S.; Suyehiro, S.; Evertson, D.W. Sacks-Evertson strainmeter, its installation in Japan and some preliminary results concerning strain steps. *Proc. Jpn. Acad.* **1971**, *47*, 707–712. [CrossRef]
59. Linde, A.T.; Agustsson, K.; Sacks, I.S.; Stefansson, R. Mechanism of the 1991 eruption of Hekla from continuous borehole strain monitoring. *Nature* **1993**, *365*, 737. [CrossRef]
60. Bonafede, M. Modelling gravity variations consistent with ground deformation in the Campi Flegrei caldera (Italy). *J. Volcanol. Geotherm. Res.* **1998**, *81*, 137–157. [CrossRef]
61. Gambino, S.; Falzone, G.; Ferro, A.; Laudani, G. Volcanic processes detected by tiltmeters: A review of experience on Sicilian volcanoes. *J. Volcanol. Geotherm. Res.* **2014**, *271*, 43–54. [CrossRef]
62. Mattia, M.; Rossi, M.; Guglielmino, F.; Aloisi, M.; Bock, Y. The shallow plumbing system of Stromboli Island as imaged from 1 Hz instantaneous GPS positions. *Geophys. Res. Lett.* **2004**, *31*, L24610. [CrossRef]
63. Mattia, M.; Aloisi, M.; Di Grazia, G.; Gambino, S.; Palano, M.; Bruno, V. Geophysical investigations of the plumbing system of Stromboli volcano (Aeolian Islands, Italy). *J. Volcanol. Geotherm. Res.* **2008**, *176*, 529–540. [CrossRef]
64. Bock, Y.; Macdonald, T.; Merts, J.H.; Bock, L.; Fayman, J.A. Epoch-by-EpochTM real-time GPS positioning in high dynamics and at extended ranges. In Proceedings of the ITEA Symposium on Test & Evaluation of Advanced Technology Systems, Lihue, Kauai, HI, USA, 2003. Available online: https://geodetics.com/epoch-by-epoch-real-time-gps-positioning-in-high-dynamics-and-at-extended-ranges/ (accessed on 1 August 2019).
65. Herring, T.A.; King, R.W.; McClusky, S.C. *Introduction to GAMIT/GLOBK, Release 10.3*; MIT: Cambridge, MA, USA, 2008.
66. Chiodini, G.; Cioni, R.; Guidi, M.; Raco, B.; Marini, L. Soil CO2 flux measurements in volcanic and geothermal areas. *Appl. Geochem.* **1998**, *13*, 543–552. [CrossRef]
67. Bertagnini, A.; Coltelli, M.; Landi, P.; Pompilio, M.; Rosi, M. Violent explosions yield new insights into dynamics of Stromboli volcano. *EOS Trans.* **1999**, *80*, 633–636. [CrossRef]
68. Tarantola, A.; Valette, B. Inverse Problems=Quest for Information. *J. Geophys.* **1982**, *50*, 159–170.

69. Inguaggiato, S.; Diliberto, I.S.; Federico, C.; Ponita, A.; Vita, F. Review of the evolution of geochemical monitoring, networks and methodologies applied to the volcanoes of the Aeolian Arc (Italy). *Earth Sci. Rev.* **2018**, *176*, 241–276. [CrossRef]
70. Andronico, D.; Corsaro, R.A.; Cristaldi, A.; Polacci, M. Characterizing high energy explosive eruptions at Stromboli volcano using multidisciplinary data: An example from the 9 January 2005 explosion. *J. Volcanol. Geotherm. Res.* **2008**, *176*, 541–550. [CrossRef]
71. Krischer, L.; Megies, T.; Barsch, R.; Beyreuther, M.; Lecocq, T.; Caudron, C.; Wassermann, J. ObsPy: A bridge for seismology into the scientific Python ecosystem. *Comput. Sci. Discov.* **2015**, *8*, 014003. [CrossRef]
72. Withers, M.; Aster, R.; Young, C.; Beiriger, J.; Harris, M.; Moore, S.; Trujillo, J. A comparison of select trigger algorithms for automated global seismic phase and event detection. *BSSA* **1998**, *88*, 96–106.
73. Borman, P. (Ed.) *New Manual of Seismological Observatory Practice (NMSOP-2; IASPEI)*; GFZ Germany Research Centre for Geosciences: Potsdam, Germany, 2012. [CrossRef]